Video Article

A High-throughput Cell Microarray Platform for Correlative Analysis of Cell Differentiation and Traction Forces

Kerim B. Kaylan[1], Andreas P. Kourouklis[1], Gregory H. Underhill[1]

[1]Department of Bioengineering, University of Illinois at Urbana–Champaign

Correspondence to: Gregory H. Underhill at gunderhi@illinois.edu

URL: https://www.jove.com/video/55362
DOI: doi:10.3791/55362

Keywords: Bioengineering, Issue 121, tissue engineering, biomaterials, biomechanics, microenvironment, cell microarrays, stem and progenitor cell biology

Date Published: 3/1/2017

Citation: Kaylan, K.B., Kourouklis, A.P., Underhill, G.H. A High-throughput Cell Microarray Platform for Correlative Analysis of Cell Differentiation and Traction Forces. *J. Vis. Exp.* (121), e55362, doi:10.3791/55362 (2017).

Abstract

Microfabricated cellular microarrays, which consist of contact-printed combinations of biomolecules on an elastic hydrogel surface, provide a tightly controlled, high-throughput engineered system for measuring the impact of arrayed biochemical signals on cell differentiation. Recent efforts using cell microarrays have demonstrated their utility for combinatorial studies in which many microenvironmental factors are presented in parallel. However, these efforts have focused primarily on investigating the effects of biochemical cues on cell responses. Here, we present a cell microarray platform with tunable material properties for evaluating both cell differentiation by immunofluorescence and biomechanical cell–substrate interactions by traction force microscopy. To do so, we have developed two different formats utilizing polyacrylamide hydrogels of varying Young's modulus fabricated on either microscope slides or glass-bottom Petri dishes. We provide best practices and troubleshooting for the fabrication of microarrays on these hydrogel substrates, the subsequent cell culture on microarrays, and the acquisition of data. This platform is well-suited for use in investigations of biological processes for which both biochemical (*e.g.*, extracellular matrix composition) and biophysical (*e.g.*, substrate stiffness) cues may play significant, intersecting roles.

Video Link

The video component of this article can be found at https://www.jove.com/video/55362/

Introduction

Interactions between cells and surrounding microenvironmental factors mediate a large variety of biological processes throughout development, homeostasis, and disease pathogenesis[1,2,3,4]. These microenvironmental interactions include delivery of soluble factors to cells, cell–matrix binding, and cell–cell interactions via ligand–receptor binding. In addition to the above biochemical considerations, biophysical parameters, such as substrate mechanical properties (*e.g.*, Young's modulus, porosity) and cell shape, and associated downstream mechanotransduction have increasingly gained recognition as key mediators of cell differentiation[5,6,7,8,9,10]. Signals resulting from these microenvironmental interactions serve as inputs to gene networks and signaling pathways. Moreover, these cell-intrinsic components also provide feedback to the microenvironment via secreted factors and matrix-degrading enzymes, completing a complex co-regulatory loop between cell-intrinsic genetic programs and cell-extrinsic microenvironmental factors[5,11,12].

The use of engineered systems for the controlled presentation of microenvironmental factors has proven useful in a range of different contexts[13,14,15]. Microfabricated systems in particular have facilitated precise spatial patterning of proteins and cells as well as highly parallelized analysis via miniaturization[13,16,17,18,19,20,21,22]. Cell microarrays represent one such microfabricated system in which combinations of biomolecules are contact-printed onto an elastic polyacrylamide hydrogel substrate[23,24,25]. The inclusion of cell-adhesive components (namely matrix proteins) enables sustained cell adhesion and culture on microarrays, which is frequently followed by downstream analysis via immunocytochemistry and fluorescent reporters. Cell microarrays have been productively directed towards attaining an improved understanding of liver cell phenotype[23,26], neural precursor differentiation[27], mammary progenitor fate decisions[28], embryonic stem cell maintenance/differentiation[23,29,30], lung cancer metastasis[31], and therapeutic response in melanoma[32]. We have recently demonstrated the use of cell microarrays for defining the role of extracellular matrix (ECM) protein composition in endoderm specification[33], liver progenitor differentiation[34,35], and lung tumor cell drug response[36]. In these works, we have focused on extending the combinatorial capabilities of the array platform and exploring the intersections of cell-intrinsic signaling with extracellular matrix composition and biomechanics. In addition, we have implemented biophysical readouts in this array platform to provide the ability to quantitatively characterize the role of cell contractility in differentiation processes[35]. To do so, we integrated traction force microscopy (TFM) with cell microarrays to enable high-throughput assessment of cell-generated traction. TFM is a widely utilized method to measure cell-generated traction forces and has provided significant insights regarding the coordination of single-cell and tissue-level function with the composition and biomechanics of the local microenvironment[37,38,39,40]. Thus, combining TFM with cell microarrays provides a high-throughput system for measuring key, physiologically relevant biophysical parameters.

The cell microarray platform described here consists of four sections: fabrication of polyacrylamide substrates, fabrication of arrays, cell culture and assay readout, and analysis of data. See **Figure 1** for a schematic summary of the first three experimental sections; see **Figure 2** for a

Copyright © 2017 Creative Commons Attribution-NonCommercial-NoDerivs 3.0 Unported License

schematic summary of the final section with a focus on analysis of immunofluorescence data. In order to adapt the cell microarray platform to studies of biomechanical cell–substrate interactions, we used polyacrylamide substrates of tunable Young's modulus but similar porosity, per Wen *et al.*[41]. To enable TFM measurements of forces exerted by cells on their substrate, we implemented a glass-bottom Petri dish format in addition to the thick glass microscope slides frequently utilized by other groups. Thus, this cell microarray platform is capable of parallel measurements of cell differentiation *via* immunofluorescence on microscope slides and cell-generated forces via TFM on separate glass-bottom dishes. We have also applied several improvements to the analytical approach commonly used with cell microarrays. Specifically, instead of parametric Z-scoring of overall island intensity, we measure single-cell intensity and apply quantile normalization in order to account for non-normal distributions and more accurately describe cellular behavior. We believe these improvements provide particular utility towards investigations of biological processes in which both biochemical and biophysical cues play significant, intersecting roles. Further, our analytical improvements enable the application of cell microarrays to studies of a range of cellular functions for which single-cell and population-level behavior diverge.

Protocol

1. Fabrication of Polyacrylamide Substrates

1. Clean glass substrates — either standard microscope slides for endpoint immunofluorescence or glass-bottom 35 mm Petri dishes for TFM — in order to ensure optimal polyacrylamide hydrogel fabrication and integrity during cell culture. Alternatively, use pre-cleaned glass substrates.
    1. Immerse glass substrates in 0.25% v/v Triton X-100 in distilled water (dH_2O). Place substrates on an orbital shaker for 30 min.
    2. Remove Triton X-100 solution and rinse substrates 5 times with dH_2O. Leave substrates immersed in the final rinse and place on an orbital shaker for 30 min.
    3. Remove dH_2O and immerse substrates in acetone. Place substrates on an orbital shaker for 30 min.
    4. Remove acetone and immerse substrates in methanol. Place substrates on an orbital shaker for 30 min.
    5. Remove methanol and rinse substrates 5 times with dH_2O. Immerse substrates in 0.05 N NaOH and place on an orbital shaker for 1 h.
    CAUTION: NaOH is highly caustic and can cause severe skin burns and eye damage. Wear protective gloves, clothing, and eye protection.
    6. Remove NaOH solution and rinse substrates 5 times with dH_2O. Use filtered compressed air to dry substrates and bake at 110 °C on a hot plate until dry (5 – 15 min). Cleaned substrates can be stored at room temperature indefinitely.

2. Silanize clean glass substrates in order to ensure attachment of the polyacrylamide hydrogel.
    1. Immerse clean glass substrates in freshly prepared 2% v/v 3-(trimethoxysilyl)propyl methacrylate (3-TPM) in ethanol. Place substrates on an orbital shaker for 30 min.
    CAUTION: 3-TPM is a combustible liquid. Keep away from heat, sparks, open flames, and hot surfaces and use only in a chemical fume hood.
    2. Remove 3-TPM solution and immerse substrates in ethanol. Place substrates on an orbital shaker for 5 min.
    3. Use filtered compressed air to dry the substrates and bake at 110 °C on a hot plate until dry (5 – 15 min). Silanized substrates can be stored at room temperature for up to 1 month.

3. Option 1: Fabricate polyacrylamide hydrogels on silanized microscope slides for endpoint immunofluorescence.
    1. Prepare a pre-polymer solution in dH_2O with the desired acrylamide/bisacrylamide percentage (w/v) ratio to fabricate substrates with Young's moduli of 4 kPa (4% acrylamide, 0.4% bisacrylamide), 13 kPa (6% acrylamide, 0.45% bisacrylamide), or 30 kPa (8% acrylamide, 0.55% bisacrylamide) and similar porosity, per Wen *et al.*[41]. Vortex solution until clear and filter with a 0.2 µm syringe. Pre-polymer solutions can be stored at 4 °C for 3 months.
    CAUTION: Exposure to acrylamide or bisacrylamide can result in acute toxicity, neurotoxicity, and irritation. Wear protective gloves, clothing, and eye protection.
    2. Prepare a photoinitiator solution of 20% w/v Irgacure 2959 in methanol. This photoinitiator solution cannot be stored and must be prepared fresh each time.
    3. Mix the pre-polymer and photoinitiator solutions in a 9:1 (pre-polymer:photoinitiator) ratio. Optionally degas with a vacuum chamber for 15 min to remove bubbles.
    4. Place silanized slides into a glass drying tray and pipet 100 µL of 9:1 pre-polymer:photoinitiator solution onto each slide. Gently cover each slide with a 22 × 60 mm coverslip while avoiding the creation of bubbles. Note that the coverslip prevents inhibition of the polymerization reaction by oxygen.
    5. Place drying tray in a UV crosslinker and expose slides to 365 nm UV A for 10 min (4 W/m^2). Optimize polymerization time as needed. Longer exposures risk difficulty removing the coverslip due to overpolymerization. Shorter exposures risk underpolymerization and low hydrogel stability.
    6. Immerse hydrogels in dH_2O for 5 min. Remove coverslips with a razor, taking care not to damage the polymerized hydrogels.
    7. Leave hydrogels in dH_2O at room temperature for 1 – 3 d, changing dH_2O daily. Dehydrate hydrogels at 50 °C on a hot plate until dry (15 – 30 min) and store at room temperature for up to 3 months.

4. Option 2: Fabricate fluorescent bead-containing polyacrylamide hydrogels on silanized 35 mm glass-bottom Petri dishes for live evaluation of cell–substrate interactions using TFM.
    1. Sonicate a stock solution of 1 µm fluorescent beads for 15 min to disperse aggregates.
    2. Prepare a pre-polymer solution in dH_2O with the desired acrylamide/bisacrylamide percentage (w/v) ratio to fabricate substrates with Young's moduli of 4 kPa (4% acrylamide, 0.4% bisacrylamide), 13 kPa (6% acrylamide, 0.45% bisacrylamide), or 30 kPa (8% acrylamide, 0.55% bisacrylamide) and similar porosity, per Wen *et al.*[41]. Vortex solution until clear and filter with a 0.2 µm syringe. Pre-polymer solutions can be stored at 4 °C for 3 months.
    CAUTION: Exposure to acrylamide or bisacrylamide can result in acute toxicity, neurotoxicity, and irritation. Wear protective gloves, clothing, and eye protection.

Copyright © 2017 Creative Commons Attribution-NonCommercial-NoDerivs 3.0 Unported License

3. Add fluorescent beads to the pre-polymer solution at a final concentration of 0.2% v/v and vortex to mix.
4. Prepare a photoinitiator solution of 20% w/v Irgacure 2959 in methanol. This photoinitiator solution cannot be stored and must be prepared fresh each time.
5. Mix the pre-polymer/bead and photoinitiator solutions in a 9:1 (pre-polymer/bead:photoinitiator) ratio. Optionally degas with a vacuum chamber for 15 min to remove bubbles.
6. Place silanized 35 mm glass-bottom Petri dishes into a glass drying tray and pipet 20 µL of 9:1 pre-polymer/bead:photoinitiator solution onto the center of each dish. Gently cover each slide with a 12 mm circular coverslip while avoiding the creation of bubbles. Note that the coverslip prevents inhibition of the polymerization reaction by oxygen.
7. In order to distribute the fluorescent beads to the surface of the hydrogel, invert the dishes and leave at room temperature for 20 min, per Knoll *et al.*[42].
8. While still inverted, expose dishes to 365 nm UV A for 10 min (4 W/m^2). Optimize polymerization time as needed. Longer exposures risk difficulty removing the coverslip due to overpolymerization. Shorter exposures risk underpolymerization and low hydrogel stability.
9. Immerse hydrogels in 0.1 M 4-(2-hydroxyethyl)-1-piperazineethanesulfonic acid (HEPES) buffer and leave at room temperature in the dark overnight. Remove coverslips carefully with a razor, taking care not to damage the polymerized hydrogels.
10. Dehydrate hydrogels at 50 °C on a hot plate until dry (15 – 30 min). Hydrogels can be stored at room temperature in the dark for 3 months.

2. Fabrication of Arrays

1. Prepare buffers to print biomolecules. Use the printing buffer appropriate to the biomolecules of interest. Growth factor (GF) printing buffer is broadly suitable for other classes of molecules, such as cell–cell ligands.
    1. To prepare 2× ECM protein printing buffer, add 164 mg of sodium acetate and 37.2 mg of ethylenediaminetetraacetic acid (EDTA) to 6 mL dH_2O. Vortex and incubate at 37 °C to thoroughly solubilize. After solubilization, add 50 µL of pre-warmed Triton X-100 and 4 mL of glycerol. Vortex and incubate at 37 °C again to solubilize. Add 40 – 80 µL of glacial acetic acid, titrating to adjust the pH to 4.8. 2× ECM protein printing buffer can be stored at 4 °C for 1 month.
    CAUTION: Acetic acid is flammable and corrosive. Wear protective gloves, clothing, and eye protection.
    2. To prepare 2× GF printing buffer, add 105.5 mg sodium acetate and 37.2 mg EDTA to 6 mL phosphate-buffered saline (PBS). Vortex and incubate at 37 °C to thoroughly solubilize. After solubilization, add 100 mg 3-[(3-cholamidopropyl)dimethylammonio]-1-propanesulfonate (CHAPS) and 4 mL of glycerol. 2× GF protein printing buffer can be stored at 4 °C for 1 month.

2. Prepare source plate.
    1. In a 384-well V-bottom microplate, combine equal volumes of 2× printing buffer with each biomolecule solution at double the target concentration.
    NOTE: An appropriate target concentration for most common ECM proteins is 250 µg/mL while target concentrations for other types of arrayed factors vary depending on retention in the hydrogel and biological function. The total volume in each well can be as low as 5 µL and need not be more than 15 µL. In addition to the biomolecule combinations of interest, include an arrayed fluorescent marker in order to facilitate downstream image analysis. Use rhodamine-conjugated dextran (2.5 mg/mL).
    2. Mix each well thoroughly by pipetting, taking care not to generate bubbles. Centrifuge the source microplate for 1 min at 100 × g. Fabricate microarrays using source plates prepared on the same day and stored at 4 °C until microarray fabrication.

3. Clean pins according to the instructions of the manufacturer before each microarray fabrication run. Load clean pins directly into the printhead of the microarrayer.
4. Prepare microarrayer and program using the manufacturer's software. Although the steps below are partly specific to the particular microarrayer used here, the operation of most microarrayers is similar.
    1. Turn on the humidifier unit, adjust the set point to 65% RH (non-condensing), and wait until the rheometer matches the set point. Place source plate in the appropriate adaptor.
    2. Dehydrate hydrogel substrates at 50 °C for 15 min and place into the appropriate adaptor. The microarrayer has adaptors for both microscope slides and microplates. For arraying 35 mm glass-bottom Petri dishes, load the dishes into a 6-well microplate and place the microplate into the microplate adaptor on the arrayer.
    3. Adjust the parameters of the program to accurately reflect the layout of the source plate, array design, and desired format (*e.g.*, microscope slide or microplate containing 35 mm Petri dishes). Include wash steps using both water and dimethyl sulfoxide (DMSO) between each condition in order to prevent carry-over and cross-contamination.
    4. Start array fabrication, checking no less frequently than once an hour that the humidity has not dropped below 65% RH (non-condensing) and that the pins are not clogged. If the humidity has dropped unexpectedly, pause arraying to fill the humidifier and clear associated tubes of condensation. If the pins are clogged, pause arraying to clean the pins or otherwise replace with pre-cleaned pins. Note that it is possible to array multiple types of biomolecules sequentially on the same substrates provided sufficient drying time (*i.e.*, 4 h to overnight).
    5. Once the program is complete, place fabricated arrays in a slide box or microplate covered with aluminum foil at room temperature and 65% RH (non-condensing) overnight. Note that it may be necessary to evaluate array quality and retention using general protein stains or immunofluorescence; see Brafman *et al.* for more details[25].

3. Cell Culture and Assay Readout

1. The day after fabrication, place arrayed substrates in 4-chambered dishes (microscope slides) or 6-well microplates (Petri dishes) and immerse in 1% v/v penicillin/streptomycin in PBS; use 4 mL for slides and 3 mL for dishes. Expose to UV C for 30 min. Exchange penicillin/streptomycin solution for cell culture media.

Copyright © 2017 Creative Commons Attribution-NonCommercial-NoDerivs 3.0 Unported License

2. Collect and count cells. Seed onto arrays at 500 × 10^3 - 2 × 10^6 cells/array at 4 mL per microscope slide and 3 mL per 35 mm Petri dish. Incubate array cultures at 37 °C and 5% CO_2 for 2 – 24 h or until the formation of well-populated cell islands. Adjust both seeding density and time as needed for your cells and particular application. Underseeding (*i.e.*, low density or seeding time) may result in poor array population and skewed biological outcomes. Overseeding (*i.e.*, high density or seeding time) may result in reduced array integrity due to island detachment.
3. After allowing for formation of cell islands, wash array cultures twice with pre-warmed cell culture media; again use 4 mL for slides and 3 mL for dishes. Optionally add appropriate controls and treatments (*e.g.*, small molecule inhibitors, growth factors, *etc.*) of interest to the biological system. Change the media of the arrays every 1 – 2 d in order to maintain the concentration of any treatments. Evaluate cell marker expression and cell function by immunofluorescence or cell–substrate interactions by TFM within 1 – 5 d of initiating array cultures — see Option 1 and Option 2 below.
4. Option 1: Perform endpoint immunofluorescence. Note that immunofluorescence of some proteins may require more stringent permeabilization using methanol, ethanol, or HCl. Due to potential damage to arrays, evaluate and optimize each permeabilization protocol before use in larger-scale experiments.
    1. Aspirate cell culture media from array slides in 4-chambered dishes and add 4 mL/slide of freshly prepared 4% v/v paraformaldehyde (PFA) in PBS. Incubate for 15 min at room temperature.
    CAUTION: Exposure to PFA can result in acute toxicity and can also irritate or corrode skin on contact. Wear protective gloves, clothing, and eye protection and use only in a chemical fume hood.
    2. Aspirate PFA solution and wash each slide 3 times with 4 mL of PBS. At this point, fixed slides can be stored at 4 °C for 1 week. It is advisable, however, to continue through immunolabeling and mounting on the same day as fixing in order to ensure array integrity.
    3. Aspirate PBS and add 4 mL/slide of 0.25% v/v Triton X-100 in PBS. Incubate for 10 min at room temperature.
    4. Aspirate Triton X-100 solution and wash each slide 3 times with 4 mL of PBS. Add 4 mL/slide of 5% v/v serum matched to the species of the secondary antibody (*e.g.*, donkey serum for donkey secondary antibodies) in PBS and incubate at room temperature for 1 h.
    5. Thoroughly remove the blocking solution from each slide. Add 500 µL/slide of primary antibody diluted in 5% v/v serum in PBS. This volume is sufficient to cover arrays for both 1 h incubations at room temperature as well as overnight incubations at 4 °C.
    6. Wash each array slide 3 times with 4 mL of PBS. Thoroughly remove the final wash and add 500 µL/slide of the appropriate secondary antibody diluted in 5% v/v serum in PBS.
    7. Wash each array slide 3 times with 4 mL of PBS. Wash briefly with dH_2O before carefully removing array slides from solution using forceps. Use a laboratory tissue to wick or dry residual dH_2O.
    8. Pipet 100 µL of mounting solution with DAPI across the slide while visually confirming complete coverage of the entire array.
    9. Place a 22 × 60 mm coverslip over the slide to mount. Seal the edges of the coverslip with clear nail polish. Store in the dark at 4 °C until imaging, no earlier than the next day.
    10. Image entire arrays using either a microarray scanner or inverted fluorescent microscope equipped with a robotic stage. Microarray scanners provide quicker readout but may require Cy3- or Cy5-compatible fluorophores and are often of limited resolution at the order of single cells (*i.e.*, 1 – 10 µm). Fluorescent microscopes provide the option to use a variety of fluorescent channels and higher resolution (<1 µm, ~ 100× total magnification) but provide slower readout depending on the quality of the robotic stage and magnification/objective.
    11. Save captured images of entire arrays from either method as TIFF files in order to prevent data compression or loss associated with other file formats (*e.g.*, JPG).

5. Option 2: Perform live evaluation of cell–substrate interactions using TFM.
    1. Prepare a solution of 1% v/v bovine serum albumin (BSA) and 1% v/v sodium dodecyl sulfate (SDS) in PBS to dissociate cells from substrates during TFM.
    2. Move 35 mm Petri dishes containing array cultures to an incubated (37 °C, 5% CO_2), inverted fluorescent microscope with a robotic stage for TFM measurements.
        1. In one dish, mark the positions (X-coordinate, Y-coordinate) and focus planes (Z-coordinate) of individual cell islands using phase contrast microscopy.
        2. Switch to far red fluorescent microscopy to visualize the beads. Return to each of the positions saved in the previous step and correct the Z-coordinate of the focus plane so that only the first layer of beads below the cell island is in focus. Save the new coordinates and proceed to automated imaging of all cell islands to capture pre-dissociation phase contrast and far red fluorescent images.
    3. Carefully add 150 µL of BSA/SDS solution to the dish and wait 5 min to allow for complete cell dissociation from substrate; monitor cell dissociation using phase contrast microscopy.
    4. After the cell islands have been dissociated from the substrate, return to the marked positions and check that the first layer of beads are still in focus. If these beads are out-of-plane due to deformation induced by cell-generated traction, then correct the Z-coordinate of the focus plane so that they are again in focus. Save the corrected Z-coordinates and repeat automated imaging of all islands to capture post-dissociation far red fluorescent images.
    5. Repeat Steps 3.5.1 – 3.5.4 for the remaining dishes.

4. Analysis of Data

1. Analysis of immunofluorescence data.
    1. Process acquired array images. Split composite array images into files containing individual channels (*i.e.*, red, blue, or green) and convert to 8-bit TIFF images[43,44]. Apply binning (*e.g.*, 2×2 or 4×4) to reduce image size to ~ 32 megapixels per channel to reduce memory requirements during downstream single-cell analysis of entire array images. See Supplemental Code File titled "array_processing.ijm" for an ImageJ macro implementation of these array processing steps.
    2. Note the coordinates in pixels of the top left, bottom left, and bottom right rhodamine-conjugated dextran markers or arrayed conditions. Use these coordinates to rotate the 8-bit TIFF images to be perfectly vertical and, later, to annotate output from the

Copyright © 2017 Creative Commons Attribution-NonCommercial-NoDerivs 3.0 Unported License

single-cell analysis with specific arrayed conditions. See Supplemental Code Files titled "rb_array_rotater.ijm", "rg_array_rotater.ijm", "rgb_array_rotater.ijm", and "array_gridding.ijm" for implementations of these array rotating and gridding steps.

3. Perform single-cell analysis of binned, rotated 8-bit TIFF images in CellProfiler (version 2.1.1)[45] using the following modules: IdentifyPrimaryObjects, IdentifySecondaryObjects, and MeasureObjectIntensity. IdentifyPrimaryObjects identifies nuclei, IdentifySecondaryObjects identifies immunolabels associated with each cell nucleus, and MeasureObjectIntensity provides quantifications for both nuclear labels and immunolabels.
    1. Output single-cell data from all three modules as a CSV file by channel using the ExportToSpreadsheet module to facilitate later downstream analysis. See Supplemental Code Files titled "b_array_image_analysis.cppipe", "gb_array_image_analysis.cppipe", "rb_array_image_analysis.cppipe", and "rgb_array_image_analysis.cppipe" for CellProfiler pipelines implementing these steps for image sets containing red, green, or blue channels.

4. To transform data to account for experimental variability and non-Gaussian single-cell distributions, apply quantile normalization by biological replicate[46]. This process generates a shared distribution across replicates and enables unbiased comparisons of changes in immunolabel intensity. Furthermore, unlike Z-scoring and other parametric methods, quantile normalization is non-parametric and does not assume a particular distribution of data, allowing for more representative analyses of single-cell behavior as a function of arrayed condition.
5. Plot data and interpret. Depending on the biological system and hypothesis, calculate and plot one or more of the following ensemble measures for each arrayed condition:
    1. Calculate and plot cells per island as a combined measure of adhesion and survival over the course of the experiment.
    2. Calculate and plot the quantile-normalized immunolabel intensity as a measure of cell fate or function.
    3. Calculate and plot the percentage of cells positive for an immunolabel as determined by intensity above a consistent threshold, usually 2 s.d. above the mean intensity of a negative control.
    4. Alternatively, plot distributions of immunolabel intensity in order to examine and categorize single-cell behavior as a function of arrayed condition. These distributions can further be characterized using measures of central tendency (mean, median, mode) and variation (variance, coefficient of variation, Fano factor) and hypothesis testing methods such as the Kolmogorov-Smirnov test.

2. Analysis of TFM data. Here is described an approach incorporating a previously developed algorithm by Butler *et al.* and Wang *et al.*[40,47].
    1. Use ImageJ to batch convert the images to 8-bit TIFF files. Apply pixel-averaged binning (*e.g.*, 2 × 2) to reduce the computational cost and time of downstream analysis. As algorithms for TFM have focused largely on single-cell analysis, the large cell–substrate interface of the islands (~ 17.5×10^3 μm^2) in comparison to the cell–substrate interface of a single cell (75 μm^2) necessitates the binning step.
    2. Input the captured phase contrast and far red fluorescent images (both pre-dissociation and post-dissociation) into a scientific programming environment such as MATLAB and process using the previously developed algorithms of Butler *et al.* and Wang *et al.*[40,47].
        1. Select three regions distant from the cell island. These regions are used to account for displacements due to image or sample drift.
        2. Provide the factor to convert from pixels to micrometers (*e.g.*, 0.454 pixels/μm), the Young's modulus of the substrate (*e.g.*, 13 kPa), and the Poisson's ratio (*e.g.*, 0.48 for the polyacrylamide gels described here).
        3. For each island, draw a boundary around the periphery to define the geometrical constraints; all forces outside of this boundary are zeroed. This constrained system is reasonable given the large distance (*i.e.*, 450 μm) between islands.

    3. Calculate the root-mean-square traction stress and contractile moment for each island. The contractile moment is a measure of the residual stress across the cell island and has been shown to reflect the strength of cell–cell interactions[48]. For each arrayed condition, average root-mean-square values over multiple islands and biological replicates and calculate associated variance for hypothesis testing. It is also possible to average the distribution of stresses or moments over many islands to provide a representative map of both measures as a function of geometry, *e.g.*, distance from the center of the island.

Representative Results

Using this platform, we investigated the role of both biochemical and biophysical cues in the fate specification of liver progenitors[34,35]. Protein A/G-conjugated Notch ligands showed improved retention and clustering in the polyacrylamide hydrogel (**Figure 3A**) and were furthermore capable of driving differentiation of liver progenitors towards a bile duct cell fate (**Figure 3B**). Using single-cell analysis, we quantified the response to the Notch ligands for the ECM proteins collagen I, collagen III, collagen IV, fibronectin, and laminin (**Figure 3C**), finding that the response of liver progenitors to the ligand depends also on the ECM context. Last, we utilized shRNA knockdown to generate liver progenitors without the ligands *Dll1* and *Jag1*. The response to the arrayed Notch ligand varied depending on the presence of either ligand, confirming that the responsiveness to the cell-extrinsic ligand is also a function of the cell-intrinsic ligand expression (**Figure 3D**). Further, we observed a distinct subpopulation of double-positive (ALB+/OPN+) cells in the *Dll1* knockdown (**Figure 3D**). Together, these representative results show: (1) the combinatorial capabilities of the array format, as exemplified by the pairing of multiple arrayed ECM proteins and Notch ligands with the knockdown of individual ligands; (2) the functionality of not only arrayed ECM proteins but also arrayed cell–cell ligand via Protein A/G-mediated conjugation; and (3) the implementation of our single-cell analysis and its ability to discern unique subpopulations.

Copyright © 2017 Creative Commons Attribution-NonCommercial-NoDerivs 3.0 Unported License

We also observed that the differentiation of liver progenitors is dependent on both the substrate stiffness and the ECM composition (**Figure 4A**), specifically finding that collagen IV is supportive of differentiation on both soft and stiff substrates while fibronectin only supports differentiation on stiff substrates (**Figure 4B**). Representative heat maps of TFM measurements suggested that sustained traction stress at low substrate stiffness on collagen IV promoted differentiation into bile duct cells (**Figure 4C**), a finding confirmed by average root-mean-square values (**Figure 4D**). Together, these representative results show: (1) the successful integration of TFM with cell microarrays on substrates with a tunable stiffness to assess both the cell phenotype and the traction stress; (2) the coordination of the liver progenitor cell fate with both the matrix composition and the substrate stiffness; and (3) the implementation of our TFM analysis and typical traction stress profiles in cell microarrays.

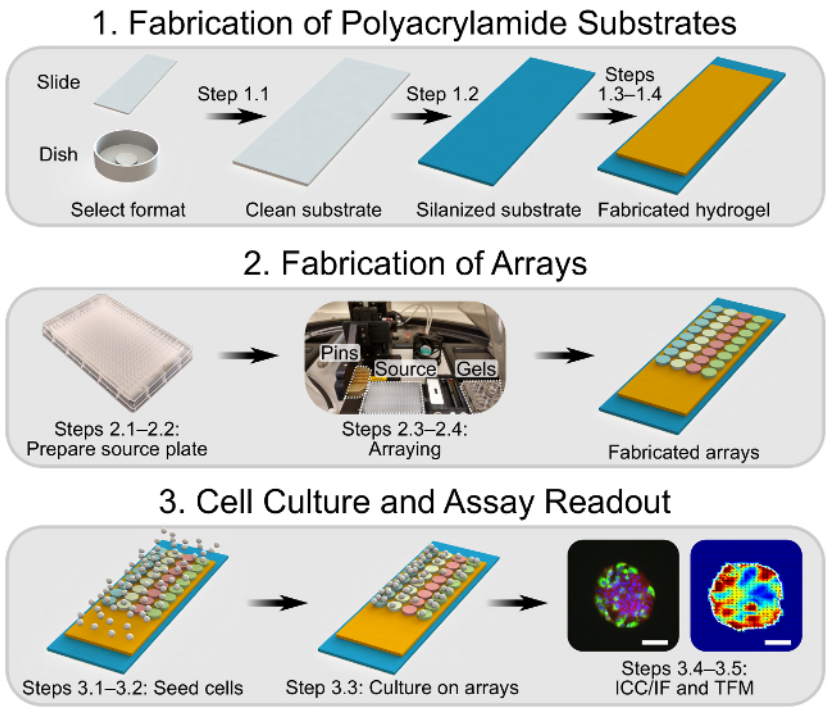

Figure 1: Overview Schematic Showing the First Three Experimental Sections. In Section 1, glass substrates are cleaned and silanized to facilitate the fabrication of polyacrylamide hydrogels. In Section 2, the biomolecule combinations of interest are prepared in a 384-well source microplate. A robotic arrayer is then loaded with clean pins, the source microplate, and the polyacrylamide hydrogels and initialized, fabricating arrays on the hydrogels. In Section 3, cells are seeded onto the arrayed domains and allowed to adhere, after which the culture protocol of interest is performed. At the endpoint, cells are either fixed for immunocytochemistry/immunofluorescence or analyzed using TFM. Scale bars are 75 µm. Please click here to view a larger version of this figure.

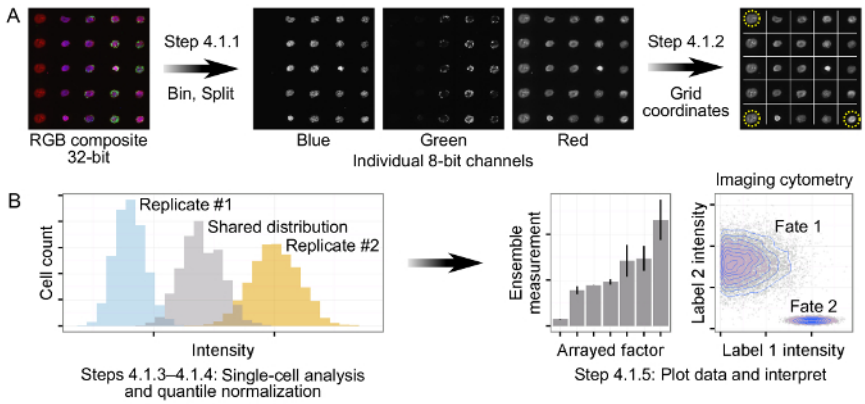

Figure 2: Processing and Analysis of Immunofluorescence Data from Arrays. (A) Tiled, composite 32-bit RGB images are first binned and then split into individual 8-bit channels. Using a combination of arrayed fluorescent markers and cell islands, three corners of the array are identified to allow for automated orientation and gridding of the arrays. **(B)** Single-cell data is generated for each channel of the input arrays. In order to account for experimental drift, quantile normalization is applied by biological replicate, producing a single shared distribution across all replicates. Quantile normalized data is subsequently plotted and interpreted via calculation of ensemble measurements (*e.g.*, cells/island, mean intensity, percentage cells positive for a label) or direct analysis of single-cell distributions. Please click here to view a larger version of this figure.

Copyright © 2017 Creative Commons Attribution-NonCommercial-NoDerivs 3.0 Unported License

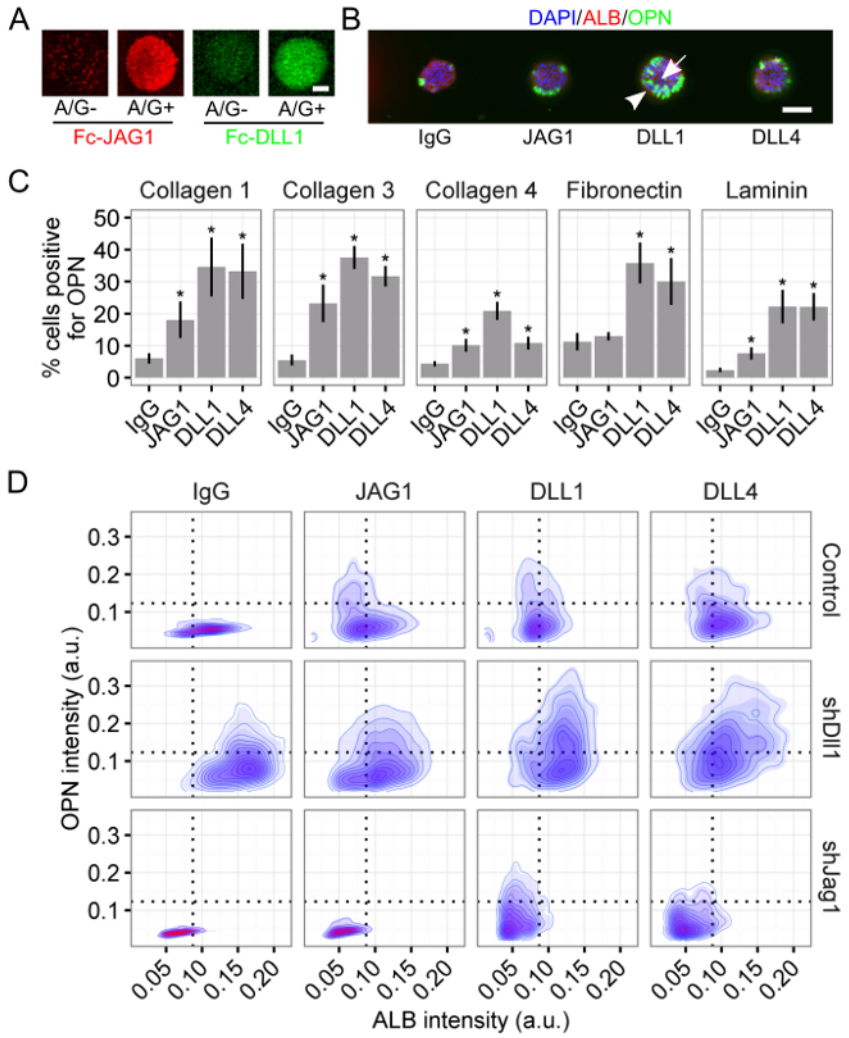

Figure 3: Notch Ligand Presentation Mediates Liver Progenitor Differentiation. (A) Fc-recombinant Notch ligands Jagged-1 (JAG1) and Delta-like 1 (DLL1) exhibited improved retention and clustering when arrayed with Protein A/G. Scale bar is 50 µm. **(B)** Liver progenitors differentiated into bile duct cells upon presentation with Notch ligand. 4',6-Diamidino-2-phenylindole (DAPI) is a nuclear label, albumin (ALB) is a hepatic cell marker, and osteopontin (OPN) is a bile duct cell marker. Scale bar is 150 µm. **(C)** Quantification of percentage of cells positive for OPN for the Notch ligands JAG1, DLL1, and Delta-like 4 (DLL4) on the ECM proteins collagen I, collagen III, collagen IV, fibronectin, and laminin. Student's *t*-tests were performed against control IgG for each arrayed Notch ligand within each ECM protein with P-values indicated for $P<0.05$ (*). **(D)** Imaging cytometry of ALB and OPN for cells on collagen III presented with the Notch ligands JAG1, DLL1, and DLL4. Liver progenitors without the Notch ligands *Dll1* and *Jag1* (*i.e.*, shDll1 and shJag1) were generated using shRNA knockdown. Data in **(C)** presented as mean ± s.e.m. This figure has been modified from Kaylan *et al.*[34]. Please click here to view a larger version of this figure.

Copyright © 2017 Creative Commons Attribution-NonCommercial-NoDerivs 3.0 Unported License

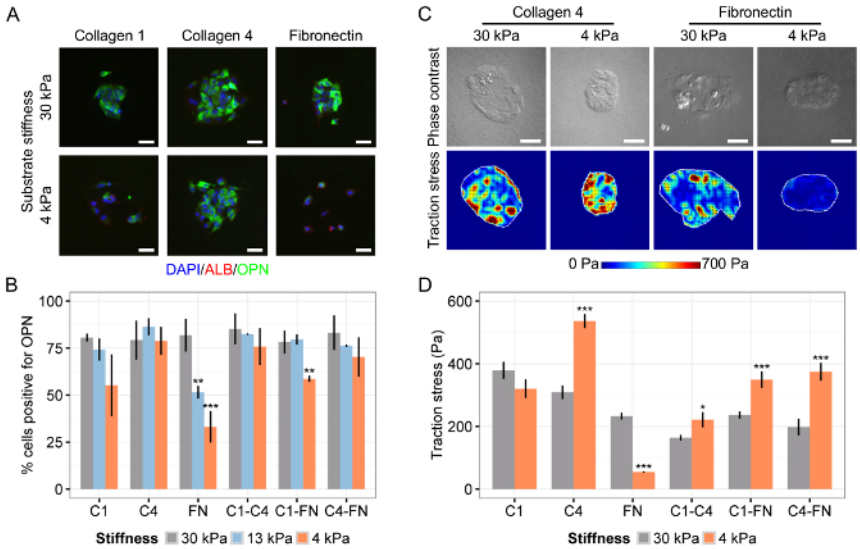

Figure 4: Matrix Composition and Substrate Stiffness Coordinate Liver Progenitor Differentiation. (A) Liver progenitor differentiation to bile duct cells is dependent on both ECM composition and substrate stiffness. DAPI is a nuclear label, ALB is a hepatic cell marker, and OPN is a bile duct cell marker. **(B)** Quantification of percentage of cells positive for OPN on substrates of Young's modulus 30 kPa, 13 kPa, and 4 kPa for collagen I (C1), collagen IV (C4), fibronectin (FN), and all two-way combinations of those ECM proteins. **(C)** Cell traction stress is dependent on both substrate stiffness and ECM composition. **(D)** Quantification of root-mean-square values of traction stress on substrates of Young's modulus 30 kPa and 4 kPa for collagen I (C1), collagen IV (C4), fibronectin (FN), and all two-way combinations of those ECM proteins. In **(B)** and **(D)**, data were presented as mean ± s.e.m and Student's *t*-tests were performed against 30 kPa for each ECM combination with P-values indicated for P< 0.05 (*), P< 0.01 (**), and P< 0.001 (***). Scale bars are 50 µm. This figure has been modified from Kourouklis *et al.*[35]. Please click here to view a larger version of this figure.

Copyright © 2017 Creative Commons Attribution-NonCommercial-NoDerivs 3.0 Unported License

Section	Problem	Potential Causes	Solution
1. Fabrication of Polyacrylamide Substrate.	Coverglass cannot be removed from hydrogel.	Overpolymerization.	Reduce polymerization time to <10 minutes (4 W/m^2). Check that UV crosslinker output is within expected range.
	Poor polyacrylamide hydrogel polymerization.	Underpolymerization.	Increase polymerization time to >10 minutes (4 W/m^2). Check that UV crosslinker output is within expected range.
	Polyacrylamide hydrogels are damaged after removal of coverglass.	Soft polyacrylamide hydrogels are easy to damage.	We observe decreasing hydrogel fabrication yield (~50%) for the softest (*i.e.*, 4 kPa) hydrogels in particular. Handle hydrogels gently and increase starting numbers to attain desired yield.
2. Fabrication of Arrays.	Poor or inconsistent spot morphology.	Inconsistent humidifier function.	Check that humidifier and rheometer a functional throughout each print run and maintain 65% RH.
		Pins stuck in printhead or clogged.	Clean the printhead to allow for free pin movement. Clean pins thoroughly before or after each print run to remove aggregates from pin channels.
3. Cell Culture and Assay Execution.	Cell detachment or death on arrays after initial attachment.	Overseeding and excessive proliferation.	Reduce initial seeding density and time. Use "maintenance" or "differentiation" media during array culture to reduce cell proliferation.
		Release of toxic acrylamide monomer from hydrogel.	Soak hydrogels in dH_2O for at least 3 d to allow for diffusion/release of acrylamide monomer and reduce cell toxicity.
	Cells don't attach to arrays.	Underseeding.	Increase initial seeding density and time. Use a more strongly adherent cell type.
		Poor deposition of matrix or biomolecule condition.	Clean pins of particles and aggregates, confirm printing parameters, and evaluate spotting of fluorescent markers, *e.g.*, rhodamine-conjugated dextran.
		Specificity of cell–matrix interactions.	Different cell types adhere specifically to some but not other ECM proteins. Test multiple different ECM proteins with your cells.
		Suboptimal array storage after fabrication.	We recommend storing fabricated arrays overnight at 65% RH and room temperature, in part to avoid phase changes during freezing. Cell adhesion is sensitive to both humidity, temperature, and storage time; make sure these parameters are consistent/optimized for your experiments.
	Detachment of hydrogel from glass substrate during cell culture.	Poor slide cleaning and silanization.	Replace working solutions for slide cleaning and silanization.
		Overdehydrated hydrogel.	Don't leave hydrogels dehydrating on a hot plate for longer than 15–30 min.
4. Analysis of Data.	High variability between replicate spots and slides.	Variability in array fabrication.	Check that pins and printhead are clean. Confirm humidifier function. Visualize and quantify spot and array quality using fluorescent markers. Store arrays as recommended above.

Table 1: Troubleshooting.

Discussion

In our experiments, we have found that the most common failures are related to the quality of fabricated arrays and poorly characterized response in the biological system of interest. We refer the reader to **Table 1** for common failure modes in cell microarray experiments and associated troubleshooting steps. Regarding quality of arrays in particular, we recommend the following. Confirm the technical quality and robustness of arraying programs, parameters, and buffers using fluorescently labeled molecules such as rhodamine-conjugated dextran. Thoroughly clean pins either before or after arraying per the manufacturer's instructions and further visually check that the pin channels are clear of debris using a light microscope. Confirm arrayed biomolecule retention using general protein stains or immunolabeling. Note that biomolecules with a molecular weight below 70 kDa are frequently not retained in the hydrogel[23,31]. Validate arrayed biomolecule cell-functionality using multiple cell types. Note that only adherent cells are compatible with arrays; additionally, adhesion to arrays is dependent on both cell-specific properties (*e.g.*, integrin expression profile) and the selected ECM proteins.

Due to limited space, we have not provided an extensive treatment of array design, layout, and fabrication here and refer the reader to previous works[23,25]. We generally use 100 spot subarrays (150 µm spot diameter, 450 µm center-to-center distance) composed of 10–20 unique biomolecule conditions (*i.e.*, 5–10 spots/condition). The number of subarrays in one array varies depending on the number of biomolecule conditions of interest, which can be comfortably scaled up to 1,280 on one 25 × 75 mm microscope slide (~ 6,400 spots in 64 subarrays)[25,31]. The parameters above will further vary depending on the pattern size of interest; pins capable of generating patterns from 75 – 450 µm are readily available.

Copyright © 2017 Creative Commons Attribution-NonCommercial-NoDerivs 3.0 Unported License

Array experiments are best complemented by validation of high-scoring arrayed conditions of interest using other culture formats, assay readouts, and biological model systems. Specifically, we recommend further validating effects of select arrayed conditions using bulk cultures in conjunction with standard molecular biology techniques (*e.g.*, qRT-PCR, immunoblotting) or standard TFM. Genetic manipulation (*e.g.*, knockdown or overexpression) of the factor of interest in an appropriate biological model system can also serve to confirm effects observed in arrays. *In vivo* animal models represent another means of validation and were recently used, for example, to confirm the central role of galectin-3 and galectin-8 in the lung cancer metastatic niche, as initially identified via cell microarray[31,49].

A number of other methods have been used to probe microenvironmental regulation of cellular functions, including a variety of two-dimensional microfabricated systems[18,50,51,52,53,54,55] and three-dimensional engineered biomaterial systems[56,57,58,59,60,61]. In comparison with other methods, the particular advantages of the cell microarray platform described here consist of: (1) throughput up to hundreds or thousands of different combinations of factors, enabling analysis of interaction effects; (2) accessible, automated imaging and analysis; (3) integration of both biochemical and biophysical readouts with controlled presentation of arrayed factors; (4) ability to vary substrate material properties; and (5) high-content single-cell analysis of cell fate and function.

In summary, the combination of cell microarrays with TFM on substrates of tunable substrate stiffness enables thorough characterization of both biochemical and biophysical cues. As presented here, this platform is generalizable and can be readily applied to a variety of adherent cell types and tissue contexts towards an improved understanding of combinatorial microenvironmental regulation of cell differentiation and mechanotransduction.

Disclosures

The authors declare that they have no competing financial interests.

Acknowledgements

We acknowledge Austin Cyphersmith and Mayandi Sivaguru (Carl R. Woese Institute for Genomic Biology, University of Illinois at Urbana–Champaign) for assistance with microscopy and for generously accommodating screen and video capture at the microscopy core.

References

1. Joyce, J. A., & Pollard, J. W. Microenvironmental regulation of metastasis. *Nat Rev Cancer.* **9**(4), 239-252 (2009).
2. Hsu, Y. C., & Fuchs, E. A family business: stem cell progeny join the niche to regulate homeostasis. *Nat Rev Mol Cell Biol.* **13**(2), 103-114 (2012).
3. Whiteside, T. L. The tumor microenvironment and its role in promoting tumor growth. *Oncogene.* **27**(45), 5904-5912 (2008).
4. Jones, D. L., & Wagers, A. J. No place like home: anatomy and function of the stem cell niche. *Nat Rev Mol Cell Biol.* **9**(1), 11-21 (2008).
5. Discher, D. E., Mooney, D. J., & Zandstra, P. W. Growth factors, matrices, and forces combine and control stem cells. *Science.* **324**(5935), 1673-1677 (2009).
6. Trappmann, B. *et al.* Extracellular-matrix tethering regulates stem-cell fate. *Nat Mater.* **11**(7), 642-649 (2012).
7. Ivanovska, I. L., Shin, J. W., Swift, J., & Discher, D. E. Stem cell mechanobiology: diverse lessons from bone marrow. *Trends Cell Biol.* **25**(9), 523-532 (2015).
8. Engler, A. J., Sen, S., Sweeney, H. L., & Discher, D. E. Matrix elasticity directs stem cell lineage specification. *Cell.* **126** (4), 677-689 (2006).
9. Chaudhuri, O. *et al.* Hydrogels with tunable stress relaxation regulate stem cell fate and activity. *Nat Mater.* **15**(3), 326-334 (2016).
10. McBeath, R., Pirone, D. M., Nelson, C. M., Bhadriraju, K., & Chen, C. S. Cell shape, cytoskeletal tension, and RhoA regulate stem cell lineage commitment. *Dev Cell.* **6**(4), 483-495 (2004).
11. Legate, K. R., Wickstrom, S. A., & Fassler, R. Genetic and cell biological analysis of integrin outside-in signaling. *Genes Dev.* **23**(4), 397-418 (2009).
12. Kessenbrock, K., Plaks, V., & Werb, Z. Matrix metalloproteinases: regulators of the tumor microenvironment. *Cell.* **141**(1), 52-67 (2010).
13. Underhill, G. H. Stem cell bioengineering at the interface of systems-based models and high-throughput platforms. *Wiley Interdiscip Rev Syst Biol Med.* **4**(6), 525-545 (2012).
14. Underhill, G. H., Galie, P., Chen, C. S., & Bhatia, S. N. Bioengineering methods for analysis of cells in vitro. *Annu Rev Cell Dev Biol.* **28** 385-410 (2012).
15. Zorlutuna, P. *et al.* Microfabricated biomaterials for engineering 3D tissues. *Adv Mater.* **24**(14), 1782-1804 (2012).
16. Ruiz, S. A., & Chen, C. S. Microcontact printing: A tool to pattern. *Soft Matter.* **3**(2), 168-177 (2007).
17. Guillotin, B., & Guillemot, F. Cell patterning technologies for organotypic tissue fabrication. *Trends Biotechnol.* **29**(4), 183-190 (2011).
18. Théry, M. Micropatterning as a tool to decipher cell morphogenesis and functions. *J. Cell Sci.* **123**(Pt 24), 4201-4213 (2010).
19. Ranga, A., & Lutolf, M. P. High-throughput approaches for the analysis of extrinsic regulators of stem cell fate. *Curr. Opin. Cell Biol.* **24**(2), 236-244 (2012).
20. Kobel, S., & Lutolf, M. High-throughput methods to define complex stem cell niches. *Biotechniques.* **48**(4), ix-xxii (2010).
21. Fernandes, T. G., Diogo, M. M., Clark, D. S., Dordick, J. S., & Cabral, J. M. S. High-throughput cellular microarray platforms: applications in drug discovery, toxicology and stem cell research. *Trends Biotechnol.* **27**(6), 342-349 (2009).
22. Montanez-Sauri, S. I., Beebe, D. J., & Sung, K. E. Microscale screening systems for 3D cellular microenvironments: platforms, advances, and challenges. *Cell Mol Life Sci.* **72**(2), 237-249 (2015).
23. Flaim, C. J., Chien, S., & Bhatia, S. N. An extracellular matrix microarray for probing cellular differentiation. *Nat Methods.* **2**(2), 119-125 (2005).
24. Underhill, G. H., Flaim, C. J., & Bhatia, S. N. in *Methods in Bioengineering: Stem Cell BioengineeringArtech House Methods in Bioengineering.* eds Biju Parekkadan & Martin Yarmush) 63-73 Artech House Publishers, Boston, MA (2009).

Copyright © 2017 Creative Commons Attribution-NonCommercial-NoDerivs 3.0 Unported License

25. Brafman, D. A., Chien, S., & Willert, K. Arrayed cellular microenvironments for identifying culture and differentiation conditions for stem, primary and rare cell populations. *Nat Protoc.* **7**(4), 703-717 (2012).
26. Brafman, D. A. *et al.* Investigating the role of the extracellular environment in modulating hepatic stellate cell biology with arrayed combinatorial microenvironments. *Integr Biol (Camb).* **1**(8-9), 513-524 (2009).
27. Soen, Y., Mori, A., Palmer, T. D., & Brown, P. O. Exploring the regulation of human neural precursor cell differentiation using arrays of signaling microenvironments. *Mol Syst Biol.* **2** 37 (2006).
28. LaBarge, M. A. *et al.* Human mammary progenitor cell fate decisions are products of interactions with combinatorial microenvironments. *Integr Biol (Camb).* **1**(1), 70-79 (2009).
29. Anderson, D. G., Levenberg, S., & Langer, R. Nanoliter-scale synthesis of arrayed biomaterials and application to human embryonic stem cells. *Nat Biotechnol.* **22**(7), 863-866 (2004).
30. Brafman, D. A., Shah, K. D., Fellner, T., Chien, S., & Willert, K. Defining long-term maintenance conditions of human embryonic stem cells with arrayed cellular microenvironment technology. *Stem Cells Dev.* **18**(8), 1141-1154 (2009).
31. Reticker-Flynn, N. E. *et al.* A combinatorial extracellular matrix platform identifies cell-extracellular matrix interactions that correlate with metastasis. *Nat Commun.* **3** 1122 (2012).
32. Wood, K. C. *et al.* MicroSCALE screening reveals genetic modifiers of therapeutic response in melanoma. *Sci Signal.* **5**(224), rs4 (2012).
33. Braga Malta, D. F. *et al.* Extracellular matrix microarrays to study inductive signaling for endoderm specification. *Acta Biomater.* **34** 30-40 (2016).
34. Kaylan, K. B., Ermilova, V., Yada, R. C., & Underhill, G. H. Combinatorial microenvironmental regulation of liver progenitor differentiation by Notch ligands, TGFbeta, and extracellular matrix. *Sci Rep.* **6**(23490), 23490 (2016).
35. Kourouklis, A. P., Kaylan, K. B., & Underhill, G. H. Substrate stiffness and matrix composition coordinately control the differentiation of liver progenitor cells. *Biomaterials.* **99** 82-94 (2016).
36. Kaylan, K. B. *et al.* Mapping lung tumor cell drug responses as a function of matrix context and genotype using cell microarrays. *Integr. Biol.* in press (2016).
37. Mann, C., & Leckband, D. Measuring Traction Forces in Long-Term Cell Cultures. *Cellular and Molecular Bioengineering.* **3**(1), 40-49 (2010).
38. Heisenberg, C. P., & Bellaiche, Y. Forces in tissue morphogenesis and patterning. *Cell.* **153**(5), 948-962 (2013).
39. Schwarz, U. S., & Soine, J. R. Traction force microscopy on soft elastic substrates: A guide to recent computational advances. *Biochim Biophys Acta.* **1853**(11 Pt B), 3095-3104 (2015).
40. Butler, J. P., Tolic-Norrelykke, I. M., Fabry, B., & Fredberg, J. J. Traction fields, moments, and strain energy that cells exert on their surroundings. *American Journal of Physiology-Cell Physiology.* **282**(3), C595-C605 (2002).
41. Wen, J. H. *et al.* Interplay of matrix stiffness and protein tethering in stem cell differentiation. *Nat Mater.* **13**(10), 979-987 (2014).
42. Knoll, S. G., Ali, M. Y., & Saif, M. T. A novel method for localizing reporter fluorescent beads near the cell culture surface for traction force microscopy. *J Vis Exp.* (91), 51873 (2014).
43. Schneider, C. A., Rasband, W. S., & Eliceiri, K. W. NIH Image to ImageJ: 25 years of image analysis. *Nat Methods.* **9**(7), 671-675 (2012).
44. Schindelin, J. *et al.* Fiji: an open-source platform for biological-image analysis. *Nat Methods.* **9**(7), 676-682 (2012).
45. Kamentsky, L. *et al.* Improved structure, function and compatibility for CellProfiler: modular high-throughput image analysis software. *Bioinformatics.* **27**(8), 1179-1180 (2011).
46. Bolstad, B. M., Irizarry, R. A., Astrand, M., & Speed, T. P. A comparison of normalization methods for high density oligonucleotide array data based on variance and bias. *Bioinformatics.* **19**(2), 185-193 (2003).
47. Wang, N. *et al.* Cell prestress. I. Stiffness and prestress are closely associated in adherent contractile cells. *Am J Physiol Cell Physiol.* **282**(3), C606-616 (2002).
48. Krishnan, R. *et al.* Substrate stiffening promotes endothelial monolayer disruption through enhanced physical forces. *Am J Physiol Cell Physiol.* **300**(1), C146-154 (2011).
49. Reticker-Flynn, N. E., & Bhatia, S. N. Aberrant glycosylation promotes lung cancer metastasis through adhesion to galectins in the metastatic niche. *Cancer Discov.* **5**(2), 168-181 (2015).
50. Chen, C. S., Mrksich, M., Huang, S., Whitesides, G. M., & Ingber, D. E. Geometric control of cell life and death. *Science.* **276**(5317), 1425-1428 (1997).
51. Kilian, K. A., Bugarija, B., Lahn, B. T., & Mrksich, M. Geometric cues for directing the differentiation of mesenchymal stem cells. *Proc Natl Acad Sci USA .* **107**(11), 4872 (2010).
52. Nelson, C. M., & Chen, C. S. Cell-cell signaling by direct contact increases cell proliferation via a PI3K-dependent signal. *FEBS Lett.* **514**(2-3), 238-242 (2002).
53. Hui, E. E., & Bhatia, S. N. Micromechanical control of cell-cell interactions. *Proc. Natl. Acad. Sci. U. S. A.* **104**(14), 5722-5726 (2007).
54. Lutolf, M. P., & Blau, H. M. Artificial stem cell niches. *Adv Mater.* **21**(32-33), 3255-3268 (2009).
55. Gobaa, S. *et al.* Artificial niche microarrays for probing single stem cell fate in high throughput. *Nat. Methods.* **8**(11), 949-955 (2011).
56. DeForest, C. A., & Anseth, K. S. Cytocompatible click-based hydrogels with dynamically tunable properties through orthogonal photoconjugation and photocleavage reactions. *Nat Chem.* **3**(12), 925-931 (2011).
57. Nelson, C. M., VanDuijn, M. M., Inman, J. L., Fletcher, D. A., & Bissell, M. J. Tissue geometry determines sites of mammary branching morphogenesis in organotypic cultures. *Sci. STKE.* **314**(5797), 298 (2006).
58. Liu Tsang, V. *et al.* Fabrication of 3D hepatic tissues by additive photopatterning of cellular hydrogels. *FASEB J.* **21**(3), 790-801 (2007).
59. Albrecht, D. R., Underhill, G. H., Mendelson, A., & Bhatia, S. N. Multiphase electropatterning of cells and biomaterials. *Lab. Chip.* **7**(6), 702-709 (2007).
60. Chan, V., Zorlutuna, P., Jeong, J. H., Kong, H., & Bashir, R. Three-dimensional photopatterning of hydrogels using stereolithography for long-term cell encapsulation. *Lab. Chip.* **10**(16), 2062-2070 (2010).
61. Boghaert, E. *et al.* Host epithelial geometry regulates breast cancer cell invasiveness. *Proc. Natl. Acad. Sci. U. S. A.* **109**(48), 19632-19637 (2012).

Copyright © 2017 Creative Commons Attribution-NonCommercial-NoDerivs 3.0 Unported License